Liquid Crystals
Publication details, including instructions for authors and subscription information:
http://www.informaworld.com/smpp/title~content=t713926090

Characterization of the B_4 phase by dielectric and AFM measurements

H. Kresse; J. Salfetnikova; H. Nadasi; W. Weissflog; A. Hauser

Online publication date: 06 August 2010

To cite this Article Kresse, H. , Salfetnikova, J. , Nadasi, H. , Weissflog, W. and Hauser, A.(2001) 'Characterization of the B_4 phase by dielectric and AFM measurements', Liquid Crystals, 28: 7, 1017 — 1023
To link to this Article: DOI: 10.1080/02678290110039093
URL: http://dx.doi.org/10.1080/02678290110039093

LIQUID CRYSTALS, 2001, VOL. 28, NO. 7, 1017–1023

Characterization of the B_4 phase by dielectric and AFM measurements

H. KRESSE*, J. SALFETNIKOVA, H. NADASI, W. WEISSFLOG and A. HAUSER

Martin-Luther-Universität Halle-Wittenberg, Institut für Physikalische Chemie, Mühlpforte 1, D-06108 Halle, Germany

(*Received 18 September 2000; accepted 11 December 2000*)

Dielectric measurements on a sample consisting of banana-shaped molecules were carried out in a frequency range between 0.1 Hz and 10 MHz. The sample exhibited B_2 and B_4 phases. As usual, two ranges of relaxation were detected in the B_2 phase, the fast reorientation about the long axes of the molecules and a slow collective process. In the B_4 phase, only one dielectric active process at low frequencies was found; this does not differ from the low frequency relaxation of the B_2 modification. This relaxation is probably related to the dynamics of superstructures. Crystallization could be observed after keeping the sample for a longer time at higher temperature. Thus, it was possible to differentiate clearly between the crystalline and the B_4 phases. AFM investigations prove the existence of focal-conic domains and periodic superstructures in the B_4 phase; then do not appear in the crystalline state. For this reason the B_4 phase is regarded as different from a classical crystalline phase.

1. Introduction

In 1996 Niori *et al.* [1] discovered the first members of a new system of mesomorphic phases formed by banana-shaped molecules and situated between the isotropic and solid states. To date, eight polymorphic phases are known and most of them have been characterized by X-ray measurements [2–4]. Link *et al.* [5] and Brand *et al.* [6] have demonstrated that there are different possibilities for the arrangement of such molecules, and so different superstructures can be formed. Dielectric investigations can help to understand the specific relations in phases resulting from bent-shaped molecules, which are in part comparable with the different modifications of the chiral smectic C phase (see for example [7]).

In previous investigations it was demonstrated that the B_1 [8], B_2 [9–11], B_3 [12], B_7 and B_8 [13] phases show typical dielectric behaviours which can be partially used as a 'fingerprint' for the different modifications. The B_4 phase was first investigated by the dielectric method in [14] and later in [15]. In the first publication, a low frequency absorption was expected, but could not clearly be proven. The existence of this relaxation was then demonstrated for a highly purified sample in [15] by heating and cooling. The sample involved did not crystallize, and so it was difficult to differentiate between a solid and the B_4 phase. In this paper, a sample is considered which exhibits the isotropic, B_2, B_4 and crystalline phase sequence. Atomic force microscopy (AFM) was used to characterize the morphological behaviour of the B_4 phase. The results are discussed with respect to results from known X-ray investigations of the same phase [3, 4].

* Author for correspondence; e-mail: kresse@chemie.uni-halle.de

2. Experimental

2.1. *Dielectric results*

As the sample, compound **1** was chosen [15]; this shows hysteresis with respect to the phase transitions. The data below were obtained by microscopic observation during cooling and heating with a rate of 5 K min^{-1}.

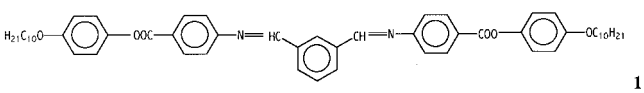

1

Cr 397 B_4 420 B_2 426 (heating); I 424 B_2 406 B_4 (cooling)

Dielectric studies were carried out in the frequency range from 0.1 Hz to 10 MHz using the Solartron Schlumberger Impedance Analyzer Si 1260 and a Chelsea Interface. A brass cell coated with gold ($d = 0.05$ mm) was used as capacitor and was calibrated with cyclohexane. The sample could not be oriented, and first measurements in the frequency range from 1 Hz to 10 MHz were made during cooling. Dielectric absorption (ε'') and dispersion (ε') curves of the two different phases are shown in figures 1 and 2.

Liquid Crystals ISSN 0267-8292 print/ISSN 1366-5855 online © 2001 Taylor & Francis Ltd
http://www.tandf.co.uk/journals
DOI: 10.1080/02678290110039093

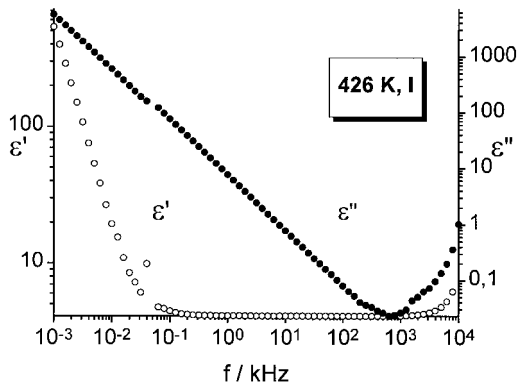

Figure 1. Dielectric constants (ε') and losses (ε'') of **1** in the isotropic (I) phase.

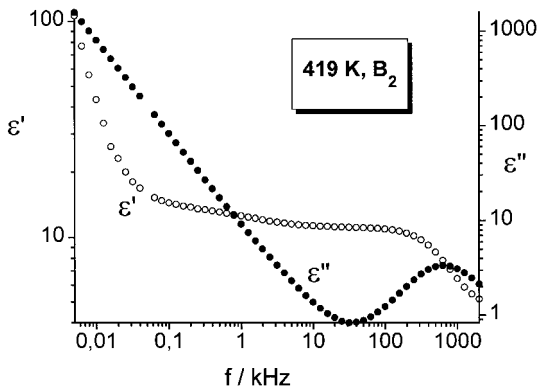

Figure 2. Dielectric constants (ε') and losses (ε'') of **1** in the B_2 phase.

The experimental data were fitted together to the real and imaginary parts of equation (1) to extract the specific behaviour of the different phases. The equation consists of two Cole–Cole mechanisms (terms 2 and 3), a conductivity contribution (term 4) and term 5 for the description of the capacitance of the double layer at low frequencies

$$\varepsilon^* = \varepsilon_2 + \frac{\varepsilon_0 - \varepsilon_1}{1 + (\mathrm{i}\omega\tau_1)^{1-\alpha_1}} + \frac{\varepsilon_1 - \varepsilon_2}{1 + (\mathrm{i}\omega\tau_2)^{1-\alpha_2}} + \frac{\mathrm{i}D}{f} + \frac{E}{f^N} \tag{1}$$

where ε_i are the low and high frequency limits of the dielectric constant, $\omega = 2\pi f$ (f is frequency), τ_i are the relaxation times, and α_i are the Cole–Cole distribution parameters; the conductivity term, as well as E and N as further fit parameters describe the capacity of the double layer. The parameter D in the conductivity term allowed us to calculate the specific conductivity σ according to

$$\sigma = D2\pi\varepsilon^0 \tag{2}$$

with $\varepsilon^0 = 8.85 \times 10^{-12}$ A s V^{-1} m^{-1}. For the low frequency mechanism, generally the limits of the dielectric constants ε_0 and ε_1 are used. For the second, the limits ε_1 and ε_2 were taken. Due to this definition, the origins of the relaxation mechanisms in the different phases must not correspond to the limits of ε_i.

The calculated limits of the dielectric constants are presented in figure 3. The B_2 phase shows the expected increase in the dielectric constants. This is partly connected with the low frequency absorption related to a collective process, but arises mainly from the high frequency absorption connected with reorientation about the molecular long axes. The strong increase in intensity at the I–B_2 transition points to the formation of ferroelectric clusters in the short range [10, 11].

For the B_4 phase, only the high frequency limit of the dielectric constants is given, as filled squares. It is important to point out that these data exceed the value of 3, but they are smaller than the high frequency limit in the B_4 phase (open triangles). A dielectric absorption in the isotropic phase could not be found within experimental error. The measured dielectric constant of about 4 in the isotropic phase indicates that there must be at least one faster motion of the molecules which should be detected in the GHz range. This should be related to the reorientation of the molecules about their long axes [9]. Analysis of the data for the low frequency collective mechanism in the B_2 phase results in distribution parameters of about $\alpha_1 = 0.25$ for the low and $\alpha_2 = 0.05$ for the high frequency process.

The specific conductivity calculated from the measured data in the range 1–100 Hz according to equation (2) is presented in figure 4. As in previous measurements [12], the conductivity decreases by about one decade at the transition into the B_4 phase. This indicates a much higher degree of limitation of the dynamics in the B_4 phase compared with the B_2 state. It is important to note that the dielectric constant in the B_4 phase remains constant for five days at room temperature and only after ten days was a small decrease in the dielectric constants detected. This gives a hint concerning the transition into the solid state.

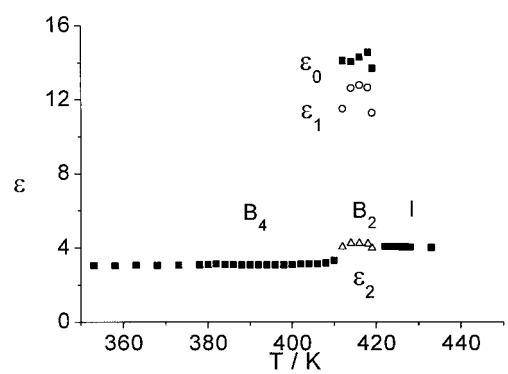

Figure 3. Limits of the dielectric constant for cooling.

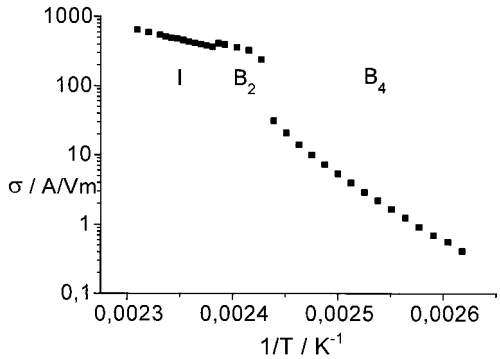

Figure 4. Specific conductivity of **1**.

After the transition into the B_4 phase, only a low frequency absorption was detected. It was difficult to extract good fit parameters from the data at low temperatures and therefore the frequency range was extended.

A second experimental run was performed during heating. At first the sample was heated to 383 K and stored for 5 hours at this temperature to transform the sample into the solid state. After that, dielectric measurements on heating were made. Dielectric data starting from 0.1 Hz in the crystalline state and after melting of the B_4 phase are shown in figures 5 and 6. The main differences between figures 5 and 6 lie in the relaxation range at 60 Hz and the higher dielectric constant in the B_4 phase. The analysis of the data results in the high frequency dielectric constants which are presented in figure 7, together with the data from figure 3 obtained during cooling. It is obvious that at $T = 397$ K the dielectric constant increases as a result of the melting process. Thus, we can conclude that in the B_4 phase dynamics of dipoles are possible. This has to take place at higher frequencies ($f > 10$ MHz) because the data given in figure 7 represent the high frequency limits of the dielectric constant in the B_4 phase and no additional relaxation could be detected in the frequency range investigated.

The stronger fluctuations of the high frequency limits in the B_4 phase result from the fitting process. The dielectric increments $\Delta_1 = \varepsilon_0 - \varepsilon_1$ of the low frequency relaxation range and the relaxation times, respectively, are presented in figures 8 and 9. With consideration of the experimental errors, we can say that the low frequency process in the B_2 and in the B_4 phase do not differ strongly from each other. The same conclusion could be reached on the homologous sample in [15]. The data obtained from the cooling and heating processes also agree well. Furthermore, there is no indication

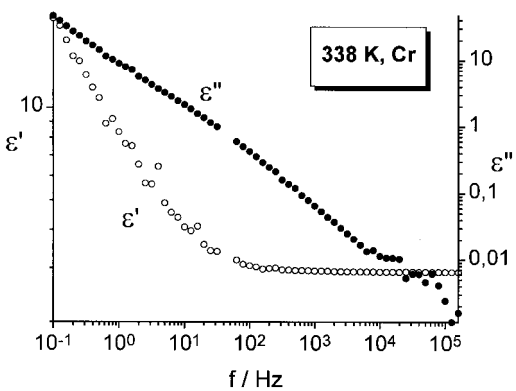

Figure 5. Dielectric data for **1** in the solid phase.

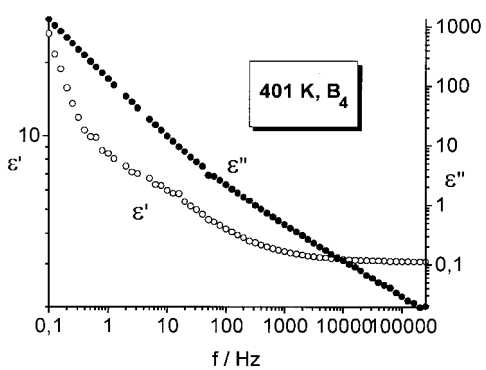

Figure 6. Dispersion and absorption in the B_4 phase.

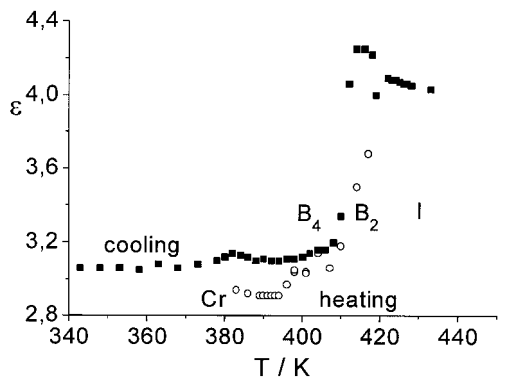

Figure 7. Calculated high frequency dielectric constants from data measured during heating and cooling.

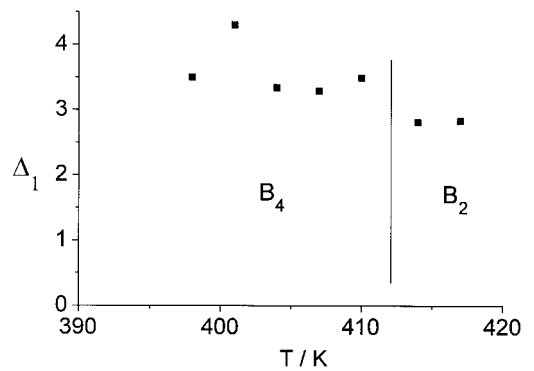

Figure 8. Dielectric increments calculated from data obtained by heating.

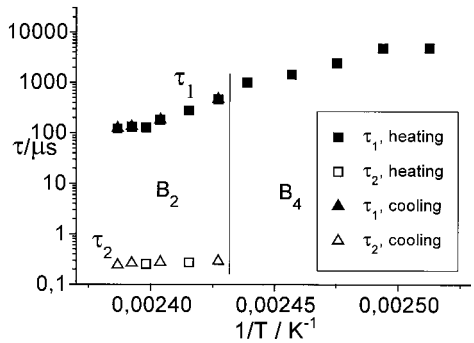

Figure 9. Relaxation times measured on heating and cooling.

that the low frequency dynamics are influenced by the phase transition: neither a critical behaviour nor a marked step in the relaxation time is seen. This points to the fact that there is no 'soft' change in the superstructure like that of the soft mode at the phase transition SmC*–SmA [7]. It has to be pointed out that the high frequency mechanism, interpreted as reorientation of the molecules about their long axes, could not be observed in the B_4 phase. Assuming a destruction of the ferroelectric short range order (decrease of intensity) and/or a much stronger hindrance of reorientation about the long axes of the molecules, it is possible that this relaxation

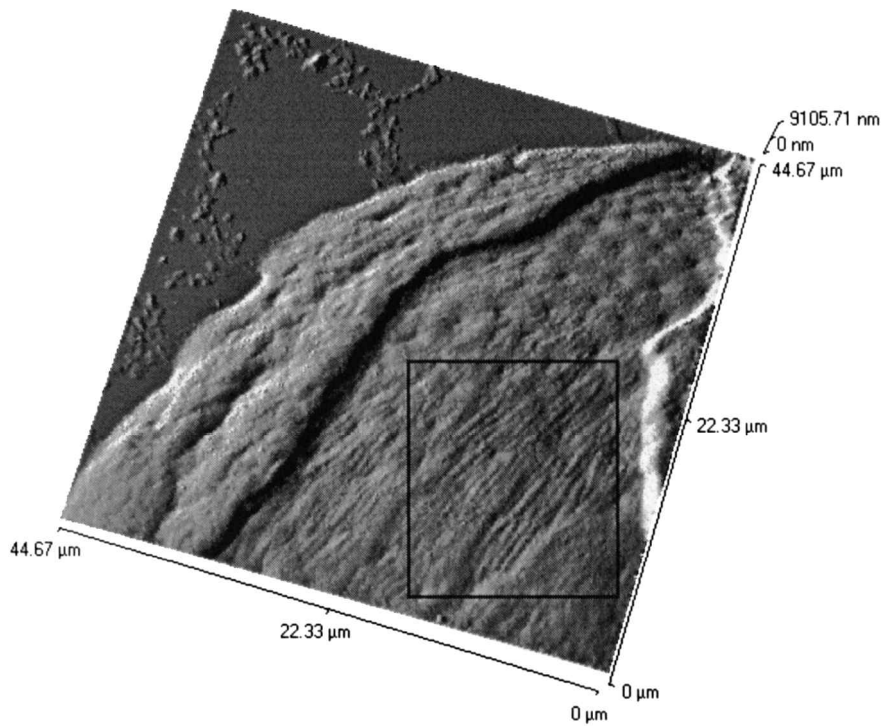

Figure 10. AFM image of a drop of the B_4 phase with focal-conic domains and periodic surface modulations (marked by a rectangle; see figure 11).

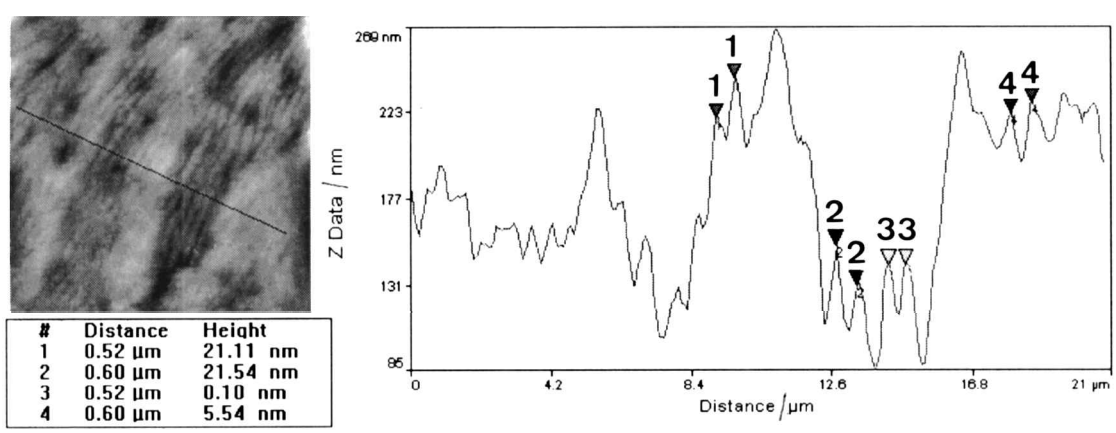

Figure 11. AFM image and line measurement of a detail from figure 10 (indicated by the rectangle) showing a periodicity of about 560 nm. The data relate to the distance and height differences between points on the line indicated by the differently numbered pairs of inverted triangles.

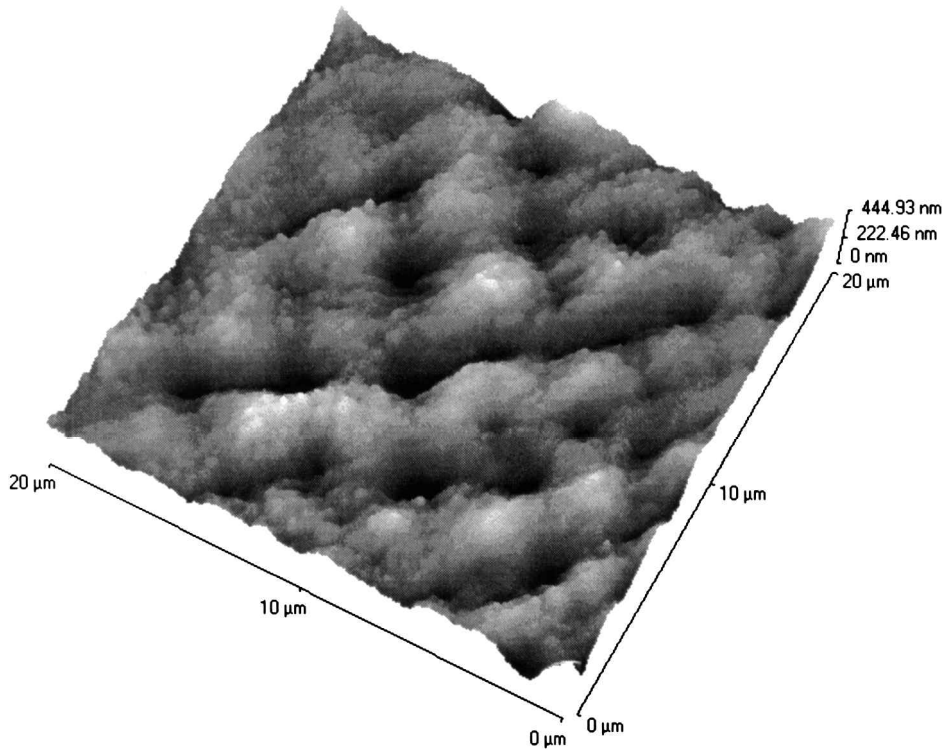

Figure 12. AFM image of the B_4 phase with lines of focal-conic domains at a distance of 4.4 µm and an additional disturbed periodicity of about 600 nm corresponding to that of figure 11.

cannot be detected experimentally. The last argument is supported by the fact that in the B_4 phase the sample becomes so firm that AFM measurements on thick samples could be performed.

2.2. *AFM investigations*

Atomic force microscopy is used to detect surface modulations caused by liquid crystalline superstructures. AFM measurements were performed at room temperature and under ambient conditions using the TMX 2010 Discoverer of Topometrix (ThermoMicroscopes) in the non-contact mode with Si-tips (161 kHz resonance frequency). The maximal scan rate was 2 Hz. The image processing used was third order plane levelling.

The samples were prepared by filling a 10 µm sandwich cell of glass with compound **1**, heating to the clearing temperature and cooling to room temperature. The cover plate was then removed and the samples were

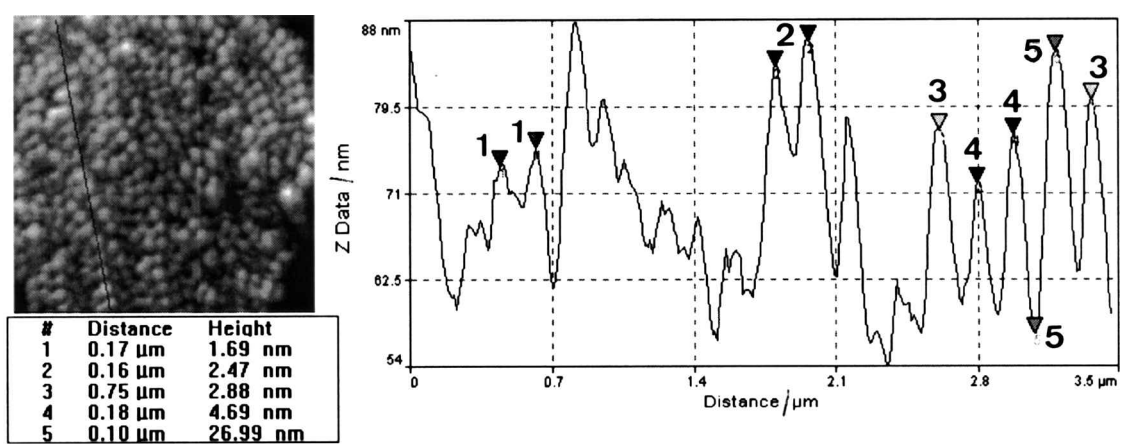

Figure 13. AFM image and line measurement of an area with a periodic surface pattern (period about 180 nm) for a sample of thickness 70 nm. The data are as described in the caption to figure 11.

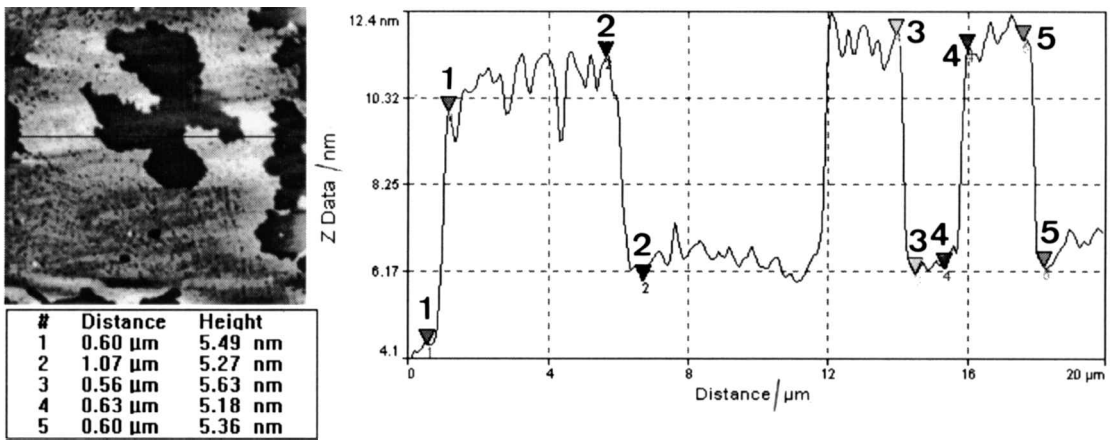

#	Distance	Height
1	0.60 µm	5.49 nm
2	1.07 µm	5.27 nm
3	0.56 µm	5.63 nm
4	0.63 µm	5.18 nm
5	0.60 µm	5.36 nm

Figure 14. AFM image and line measurement of a monolayer area of the sample with a layer thickness of about 5.4 nm. The data are as described in the caption to figure 11.

again heated to the clearing temperature and cooled to room temperature using a cooling rate of 0.5 K min^{-1} in the neighbourhood of the clearing temperature, and then to the B_4 phase at a cooling rate of 5 K min^{-1}. A sudden phase transition from B_2 to B_4 was observed by optical microscopy. The B_4 phase was then rapidly cooled to room temperature.

Figure 10 shows the AFM image of a drop with a weak focal-conic surface texture and an additional superstructure periodicity visible in the area indicated by the rectangle.

Line measurements in the area of the superstructure reveal a periodicity of about 560 nm with a modulation of height of 40 nm (figure 11). It was found that in other preparations there were regions of a few parallel 0.6 µm lines where the direction of the lines changed from region to region. Thus, the origin of this periodicity cannot be related to the scanning process. On other regions of sample, this periodicity is partly suppressed by the focal-conic domains (figure 12). Such more pronounced focal-conic domains are shown in figure 12. This texture is typical for phases ordered in layers, e.g. liquid crystalline modifications [16]. Focal-conic domains were also observed by AFM in liquid crystalline B_2 and B_7 phases [17]. The funnel-shaped centres of the focal-conic domains are in keeping with a distance between the lines of 4.4 µm (see figure 12). The difference in the height between the lines and the minimum of a funnel of the

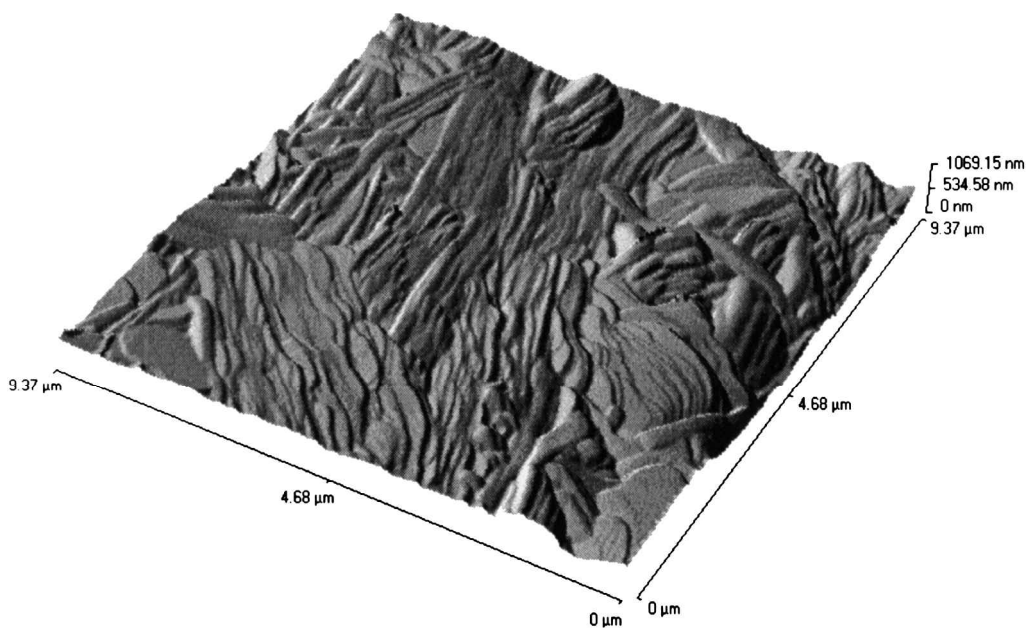

Figure 15. AFM image of the crystallized sample.

focal-conic domain was measured in some samples to be more than 1 μm.

With higher magnification on sample areas with a thickness of about 70 nm an additional periodicity of about 180 nm in distance and 25 nm in height is recognisable (see figure 13). On a sample area with only a monolayer, a layer thickness of 5.4 nm was measured (figure 14). This distance corresponds to the length of the given molecule **1**. All the distances could be reproduced over different parts of the sample and even by changing the conditions for preparation.

After annealing the sample for 2 h at 100°C in the B_4 phase, the sample crystallized. An AFM image of the crystalline surface is given in figure 15. Focal-conic domains do not appear on the crystallized sample, for which totally different surface structures are found.

In conclusion one can say that at present the experimental data for the B_4 phase have to be discussed in contradictory terms. With respect to the X-ray pattern, which exhibits in the wide angle regions several diffuse bands [3, 4], the structure has to be discussed as solid-like, with the small particle size causing the broadening of the reflections. From the measurements presented here it can be concluded that the B_4 phase does not behave from a dynamical and morphological point of view like a classical crystal with a long range three-dimensional order and completely frozen dynamics. Thus, the B_4 phase seems to be a further example lying between high temperature liquid crystals and crystalline solids.

The authors are indebted to Dr Diele for discussions as well as the DFG and the Fonds der Chemischen Industrie for financial support.

References

[1] Niori, T., Sekine, J., Watanabe, J., Furukawa, T., and Takezoe, H., 1996, *J. mater. Chem.*, **6,** 231.
[2] Watanabe, J., Niori, T., Sekine, J., and Takezoe, H., 1998, *Jpn. J. appl. Phys.*, **37,** L 139.
[3] Diele, S., Pelzl, G., and Weissflog, W., 1999, *Liq. Cryst. Today*, **9,** 8.
[4] Pelzl, G., Diele, S., and Weissflog, W., 1999, *Adv. Mater.*, **11,** 707.
[5] Link, D. R., Natale, G., Shao, R., McLennan, J. E., Clark, N. A., Körblova, E., and Walba, D. M., 1997, *Science*, **278,** 1924.
[6] Brand, H. R., Cladis, P., and Pleiner, H., 1998, *Eur. Phys. J. B*, **6,** 347.
[7] Bourney, V., Pavel, J., Lorman, V., and Nguyen, H. T., 2000, *Liq. Cryst.*, **27,** 559.
[8] Schmalfuss, H., Shen, D., Tschierske, C., and Kresse, H., 2000, *Liq. Cryst.*, **27,** 1235.
[9] Weissflog, W., Lischka, Ch., Diele, S. Pelzl, G., Wirth, I., Grande, S., Kresse, H., Schmalfuss, H., Hartung, H., and Stettler, A., 1999, *Mol. Cryst. liq. Cryst.*, **333,** 203.
[10] Schmalfuss, H., Shen, D., Tschierske, C., and Kresse, H., 1999, *Liq. Cryst.*, **26,** 1767.
[11] Schmalfuss, H., Weissflog, W., Hauser, A., and Kresse, H., 2000, *Proc. SPIE*, **4147,** 172.
[12] Salfetnikova, J., Schmalfuss, H., Nadasi, H., Weissflog, W., and Kresse, H., 2000, *Liq. Cryst.*, **27,** 1663.
[13] Schmalfuss, H., Hauser, A., and Kresse, H., *Mol. Cryst. liq. Cryst.* (in the press).
[14] Schmalfuss, H., Weissflog, W., Hauser, A., and Kresse, H., *Mol. Cryst. liq. Cryst.* (in the press).
[15] Nadasi, H., Lischka, Ch., Kresse, H., Wirth, I., Diele, S., Pelzl, G., and Weissflog, W., submitted.
[16] Bouligand, Y., 1998, *Handbook of Liquid Crystals*, Vol. 1, edited by D. Demus, J. Goodby, G. W. Gray, H.-W. Spiess and V. Vill (Weinheim: Wiley-VCH), pp. 406–453.
[17] Hauser, A., Schmalfuss, H., and Kresse, H., 2000, *Liq. Cryst.*, **27,** 629.